Su *et al.*
Chinese Journal of Mechanical Engineering (2023) 36:94
https://doi.org/10.1186/s10033-023-00929-y

Chinese Journal of Mechanical Engineering

ORIGINAL ARTICLE

Open Access

Assessment of Lubrication Property and Machining Performance of Nanofluid Composite Electrostatic Spraying (NCES) Using Different Types of Vegetable Oils as Base Fluids of External Fluid

Yu Su[1*], Zepeng Chu[1], Le Gong[1], Bin Wang[1] and Zhiqiang Liu[1]

Abstract

The current study of minimum quantity lubrication (MQL) concentrates on its performance improvement. By contrast with nanofluid MQL and electrostatic atomization (EA), the proposed nanofluid composite electrostatic spraying (NCES) can enhance the performance of MQL more comprehensively. However, it is largely influenced by the base fluid of external fluid. In this paper, the lubrication property and machining performance of NCES with different types of vegetable oils (castor, palm, soybean, rapeseed, and LB2000 oil) as the base fluids of external fluid were compared and evaluated by friction and milling tests under different flow ratios of external and internal fluids. The spraying current and electrowetting angle were tested to analyze the influence of vegetable oil type as the base fluid of external fluid on NCES performances. The friction test results show that relative to NCES with other vegetable oils as the base fluids of external fluid, NCES with LB2000 as the base fluid of external fluid reduced the friction coefficient and wear loss by 9.4%-27.7% and 7.6%-26.5%, respectively. The milling test results display that the milling force and milling temperature for NCES with LB2000 as the base fluid of external fluid were 1.4%-13.2% and 3.6%-11.2% lower than those for NCES with other vegetable oils as the base fluids of external fluid, respectively. When LB2000/multi-walled carbon nanotube (MWCNT) water-based nanofluid was used as the external/internal fluid and the flow ratio of external and internal fluids was 2:1, NCES showed the best milling performance. This study provides theoretical and technical support for the selection of the base fluid of NCES external fluid.

Keywords Nanofluid composite electrostatic spraying, Lubrication property, Machining performance, Vegetable oil, External fluid

1 Introduction

Cutting fluid mainly has three functions: cooling, lubrication and chip removal. In the process of metal cutting, a large amount of cutting fluid is often used to prolong the service life of tools and improve the machining quality of workpieces [1–5]. However, the extensive use of cutting fluid not only increases the processing cost, but also pollutes the environment, and causes serious harm to the health of operators, which is contrary to the goal of sustainable development [6, 7]. In order to reduce the use of cutting fluid, clean machining technology has been widely studied. Minimum quantity lubrication (MQL) is a quasi dry cutting technology that atomizes a small amount of lubricant by compressed air, and sprays

*Correspondence:
Yu Su
suyuliu@sohu.com; yusu20000@163.com
[1] College of Mechanical Engineering, Jiangsu University of Science and Technology, Zhenjiang 212100, China

it to the processing area so as to implement cooling and lubrication. Compared with pouring cooling, MQL technology greatly reduces the use of cutting fluid on the premise of effectively improving cutting performance. As a typical representative of clean machining technology, it has been widely used in different processing methods of different materials [8–11].

Compared with mineral oil, vegetable oil has the advantages of green and sustainable. A large number of ester groups and hydroxyl groups contained in it are strong polar groups, which can produce better affinity with the metal surface. A layer of physically adsorbed molecular film is formed between the workpiece and the tool through the Van der Waals force, effectively reducing friction and wear. And these polar molecules can react with the metal surface under certain conditions to form a chemical adsorption film, which makes the lubrication better [9, 12–14]. Therefore, vegetable oil has been more and more used in MQL to further improve its greenness. Wang et al. [14] evaluated the friction performance of grinding wheel/workpiece interface under the conditions of pouring cooling and vegetable oil-based MQL with corn oil, soybean oil, peanut oil, castor oil, rapeseed oil, palm oil, and sunflower oil as the base oil by grinding tests, and found that vegetable oil-based MQL grinding could obtain a smaller friction coefficient, and the best lubricating performance was exhibited by vegetable oil-based MQL with castor oil as the base oil. Deiab et al. [15] carried out turning tests of titanium alloy under the conditions of dry cutting, pouring cooling, liquid nitrogen cooling, rapeseed oil MQL, cold air, and rapeseed oil MQL combined with cold air, and studied the effects of cooling and lubrication conditions on surface roughness, flank wear and cutting energy consumption. They found that rapeseed oil MQL and rapeseed oil MQL combined with cold air could be used as an alternative cooling and lubrication technology for pouring cooling. Elmunafi et al. [16] performed turning tests of hardened stainless steel, and compared the cutting performance of dry cutting and vegetable oil-based MQL with castor oil as the base oil. The results showed that castor oil MQL could improve the tool life and surface roughness, and reduce the cutting force. Li et al. [17] used castor oil, soybean oil, rapeseed oil, corn oil, sunflower oil, peanut oil, and palm oil as MQL base oils to conduct the surface grinding of nickel base superalloys, and compared the grinding force, grinding temperature and energy ratio coefficient of seven vegetable oils. It was found that palm oil was the best base oil of MQL, and the vegetable oil with high viscosity presented stronger lubricating ability and lower heat exchange ability, reducing the grinding force and increasing the grinding temperature. Although vegetable oil-based MQL has many advantages, it also has some defects, namely, insufficient cooling performance and environmental and human health hazards caused by the dispersion of mist particles to the surrounding environment during oil mist transportation [1, 11, 18, 19].

Nanofluid is a two-phase suspension fluid formed by dispersing a small amount of nanoparticles to the base fluid. Based on the enhanced heat transfer theory, it can be learned that solids have higher thermal conductivity than liquids. In this way, adding nanoparticles to vegetable oil will help to improve the poor cooling capacity of vegetable oil. In addition, due to the rolling, polishing, filling effect, and the formation of lubricating film, the addition of nanoparticles to vegetable oil can also improve the tribological properties of vegetable oil [12, 20]. Therefore, in recent years, vegetable oil-based nanofluid MQL has been widely studied and encouraging results have been achieved. Manojkumar and Ghosh [21] prepared the multi-walled carbon nanotube (MWCNT)-sunflower oil nanofluid, and studied the effect of sunflower oil-based nanofluid MQL on the grinding performance of AISI 52100 steel. The results showed that compared with sunflower oil, the thermal conductivity, wettability and friction resistance of MWCNT-sunflower oil nanofluid were significantly improved. Compared with sunflower oil MQL, sunflower oil-based nanofluid MQL could more effectively maintain the sharpness of grinding wheel and reduce the wear of grinding wheel. Zhang et al. [22] studied the cooling performance of different vegetable oil-based nanofluid MQL grinding using the friction coefficient, specific friction energy, grinding temperature, and total heat flux as evaluation parameters, and analyzed the influence of physical properties of vegetable oil-based nanofluids on the cooling effect of nanofluid MQL grinding. It was found that the cooling performance of vegetable oil-based nanofluid was better than that of mineral oil due to the presence of fatty acid molecules. The lowest grinding temperature could be obtained when palm oil-based nanofluid MQL was applied. They also investigated the effects of base oil type (rapeseed oil, palm oil and soybean oil) of vegetable oil-based nanofluid MQL and mass fraction of MoS_2 nanoparticles on the grinding properties of 45 steel. The results indicated that soybean oil was the best base oil to ensure the cooling and lubricating capacity of vegetable oil-based nanofluid MQL at the same time. As the excessive mass fraction of MoS_2 led to the agglomeration of nanoparticles and then reduced the lubrication performance of nanofluid MQL, the friction coefficient and specific grinding energy first decreased and then increased with the increase of the mass fraction of MoS_2 nanoparticles [23]. Yuan et al. [24] prepared nanofluids with nanoparticles of different hardness (copper, silicon carbide and diamond) and vegetable oils with different viscosity (soybean oil, rapeseed oil and

natural 77 oil), and evaluated the processing performance of nanofluid MQL with different matches of nanoparticle hardness and base oil viscosity in end milling of 7050 aluminum alloy. They found that the rapeseed oil-based diamond nanofluid MQL and natural 77 oil-based diamond nanofluid MQL might obtain the lowest cutting force and surface roughness, respectively. Pal et al. [25] compared the drilling performance of AISI 321 stainless steel under the conditions of sunflower oil MQL and graphene-sunflower oil nanofluid MQL with different mass fractions, and found that compared with sunflower oil MQL, graphene-sunflower oil nanofluid MQL might reduce the drilling axial force, torque, surface roughness, and friction coefficient, improve the tool life, and better results could be achieved with the increase of graphene mass fraction. Singh et al. [26] conducted grinding comparative tests of titanium alloys under twenty cooling and lubrication conditions, such as dry grinding, pouring cooling, different vegetable oil-based MQL and graphene-vegetable oil nanofluid MQL with different mass fractions. The results showed that the grinding performance of vegetable oil-based nanofluid MQL was better than that of pouring cooling, and graphene-rapeseed oil nanofluid MQL with a mass fraction of 1.5% presented the best grinding performance. Su et al. [27] prepared graphite oil-based nanofluids with LB2000 vegetable oil and PriEco6000 ester oil as base fluids by a two-step method, and compared the turning force and temperature of AISI 1045 under dry cutting, MQL (LB2000, PriEco6000), and graphite oil-based nanofluid MQL (graphite-LB2000 nanofluid, graphite-PriEco6000 nanofluid). The results suggested that the graphite oil-based nanofluid MQL could significantly reduce the turning force and temperature, and LB2000 vegetable oil was suitable as the base oil for the graphite oil-based nanofluid MQL processing. Although the application of vegetable oil-based nanofluids in MQL makes up for the lack of cooling capacity of vegetable oil-based MQL, the environmental problems caused by droplet dispersion when oil mist is transported to the processing area are still unavoidable [1].

To efficiently transport droplets during processing, some researchers have investigated the electrostatic atomization (EA) processing technique. Reddy et al. [28, 29] and Su et al. [30] respectively studied the feasibility of applying EA in machining through drilling and milling experiments. It was found that compared with pouring cooling and MQL, EA might not only effectively improve the drilling and milling performance, but also greatly reduce the dispersion of droplets to the working environment and improve the air quality, due to the directional transport of droplets to the processing area. Composite electrostatic spraying (CES) is a process in which two immiscible fluids form a composite jet under a high-voltage electrostatic field, and are broken into composite droplets at the end of the composite jet. Based on the CES principle, the authors put forward a CES cutting method, and constructed a corresponding cutting experimental platform. They conducted titanium alloy milling experiments and air quality inspections under the condition of CES with LB2000 vegetable oil and water as the external and internal fluids, and investigated the feasibility of applying CES in machining. It was found that compared with EA, CES not only improved the milling performance due to the synergistic cooling and lubrication effect of external and internal fluids, but also further reduced the oil mist concentration in the working environment [31]. Further, they also proposed a nanofluid composite electrostatic spraying (NCES) cutting method, and evaluated the milling and environmental performances of NCES under four external/internal fluid combinations, namely, LB2000/water, LB2000/MWCNT water-based nanofluid, MWCNT-LB2000 nanofluid/water, and MWCNT-LB2000 nanofluid/MWCNT water-based nanofluid, and found that LB2000/MWCNT water-based nanofluid was the best external/internal fluid combination for NCES milling [32]. The current research shows that NCES can effectively improve the cooling/lubrication and environmental performances of MQL at the same time. And it is expected to become a new generation of green quasi dry cutting technology. Different base fluids of external fluid contribute different lubrication properties and machining performances of NCES. So it is very necessary to explore the suitable base fluid of external fluid for NCES. However, the research on this aspect is still blank. This paper attempted to investigate the lubrication property and machining performance of NCES with different vegetable oils as the base fluids of external fluid by friction and cutting tests under different flow ratios of external and internal fluids. And the spraying current of NCES and the electrowetting angle of composite droplets were measured so as to discuss the effect of vegetable oil type as the base fluid of external fluid on NCES performances.

2 NCES Cutting Method

Figure 1 shows the schematic diagram of NCES cutting system. The external fluid (oil or oil-based nanofluid) and the internal fluid (water or water-based nanofluid) are respectively transported to the coaxial nozzle connected to the negative pole of high voltage supply unit through the syringe pumps, and charged through contact charging. Because the electrostatic relaxation time of internal fluid is much lower than that of external fluid, the charge is distributed on the interface between them [33]. Under the action of a high-voltage electrostatic field

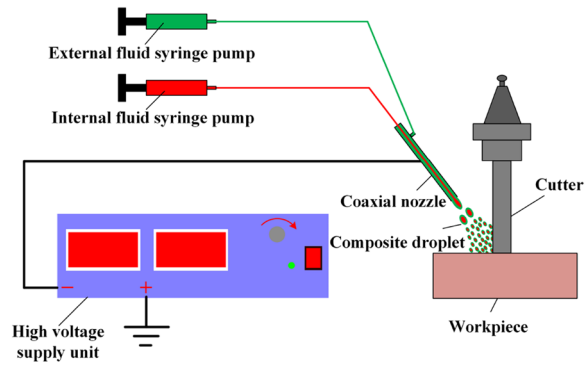

Figure 1 NCES cutting system

among coaxial nozzle, cutter and workpiece, the internal fluid drives the external fluid to form a composite jet. The charged composite droplets generated at the end of the composite jet are transported to the processing area by the electric field force. After composite droplets reach the surfaces of cutter and workpiece, the water droplets vaporize and take away part of the cutting heat. The oil film plays a lubricating role between cutter and workpiece. And nanoparticles cooperate with the oil film and water droplets to conduct heat transfer and friction reduction, thus providing efficient cooling and lubrication for the processing area.

3 Experimental Details

3.1 Preparation and Physical Property Test of Nanofluids

MWCNT with a diameter of 10–20 nm and a length of less than 2 μm was used as nanoparticles, and deionized water, castor oil, palm oil, soybean oil, rapeseed oil, and LB2000 oil were used as base fluids. Oil-based and water-based nanofluids with a volume fraction of 0.1% were prepared by a two-step method. The volume fraction needed to be converted to mass fraction before preparation. The corresponding mass of nanoparticles and base fluids was weighed using an FA2004B electronic analytical balance, and then the nanoparticles were dispersed into the base fluids using an ultrasonic cleaning machine with 100 W ultrasonic power and 2 h vibration time. In the preparation of MWCNT water-based nanofluids, it was necessary to add 0.15% by mass of gum arabic to obtain good dispersion stability.

In this study, the external fluid used was castor oil, palm oil, soybean oil, rapeseed oil, LB2000 oil, and the prepared oil-based nanofluid with a volume fraction of 0.1%, while the internal fluid used was deionized water and the prepared water-based nanofluid with a volume fraction of 0.1%. NDJ-9S rotational viscometer and BZY-1 automatic surface tensiometer were used to measure the viscosity, surface tension and interfacial tension of external and internal fluids, respectively. The measurement results are shown in Tables 1 and 2. Twenty external/internal fluid combinations listed in Table 2 were used in all tests of this study.

Table 1 Physical parameters of external and internal fluids

Fluid type	Surface tension(mN/m)	Viscosity (mPa·s)
Water	73	1
Water-based nanofluid (Water nano)	70	1.5
Castor oil (Castor)	45	550
Castor oil-based nanofluid (Castor nano)	43.5	560
Palm oil (Palm)	32.6	53
Palm oil-based nanofluid (Palm nano)	31.9	56.5
Soybean oil (Soybean)	32.6	51
Soybean oil-based nanofluid (Soybean nano)	31.8	54.4
Rapeseed oil (Rapeseed)	32.1	50
Rapeseed oil-based nanofluid (Rapeseed nano)	31.3	54
LB2000	32	52
LB2000 oil-based nanofluid (LB2000 nano)	30.5	56

Table 2 Interfacial tension between external and internal fluids

External/internal fluid combination	Interfacial tension (mN/m)
Castor/water	31.5
Castor nano/water	29.6
Castor/water nano	30.2
Castor nano/water nano	28.4
Palm/water	17.5
Palm nano/water	14.6
Palm/water nano	15.7
Palm nano/water nano	14.4
Soybean/water	17.4
Soybean nano/water	14.3
Soybean/water nano	16.3
Soybean nano/water nano	13.2
Rapeseed/water	23.6
Rapeseed nano/water	20.6
Rapeseed/water nano	23.3
Rapeseed nano/water nano	20.4
LB2000/water	19.9
LB2000 nano/water	16.3
LB2000/water nano	18.7
LB2000 nano/water nano	14.2

3.2 Test of Spraying Current and Electrowetting Angle

NCES exhibited four spraying modes: drip, pulsation, cone jet, and instability. The cone jet mode could form a continuous jet, which was suitable for cooling and lubrication during processing [34]. The previously developed spraying test platform, which involved an NCES cutting system and video microscope [32, 34], was utilized to inspect the spraying morphology of NCES with twenty external/internal fluid combinations. And the voltage range for each external/internal fluid combination to form the cone jet mode was determined under the given flow rate of external and internal fluids. Figure 2 shows the NCES charging test platform. As shown in Figure 2, the coaxial nozzle was installed on the adjustable bracket. The current collecting end of the picoammeter was connected to the metal plate through the wire, and the communication end was connected with the computer. Under the cone jet mode, the spraying current was measured with the picoammeter, and the standard deviation of spraying current was calculated. The spraying current characterized the NCES charging performance. With the increase of spraying current, the charging performance was improved, which tended to improve the spraying effect of NCES. The standard deviation of spraying current reflected the variation amplitude of spraying current and characterized the stability of spraying process. The smaller the standard deviation of spraying current, the more stable the spraying process.

Wetting angle was usually used to characterize wetting performance. Figure 3 shows the electrowetting angle measurement platform. The coaxial nozzle was perpendicular to the toughened film, and the distance between the nozzle outlet and the toughened film was 20 mm. The electrode needle connected with the negative pole of the high voltage supply unit was placed 3 mm above the toughened film in parallel, and the distance between the needle tip and the axis of the coaxial nozzle was 10 mm. The electrowetting process of the composite droplet was photographed by a horizontal video microscope, and the electrowetting angle at the stable wetting was measured.

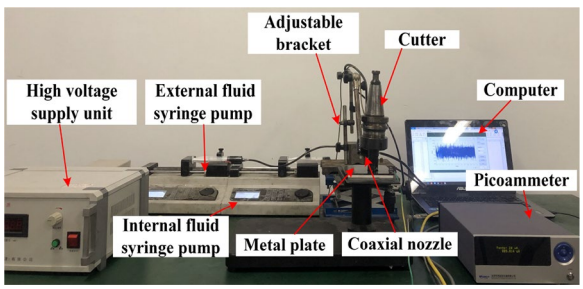

Figure 2 NCES charging test platform

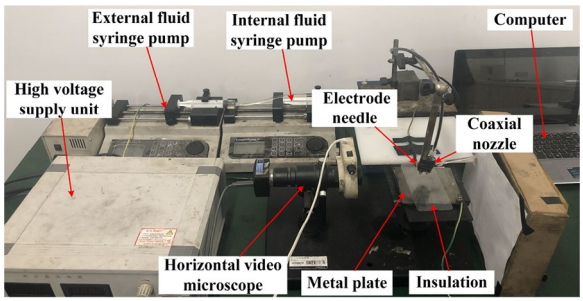

Figure 3 Electrowetting angle measurement platform

The test conditions of spraying current and electrowetting angle are shown in Table 3, where −6.5kV was the common voltage of the cone jet for twenty external/internal fluid combinations under three flow ratios of external and internal fluids. For each vegetable oil as the base fluid of external fluid, there are four external/internal fluid combinations, namely, oil/water, oil-based nanofluid/water, oil/water-based nanofluid, and oil-based nanofluid/water-based nanofluid. The average value of spraying current, standard deviation and electrowetting angle for four external/internal fluid combinations under the employed flow ratio of external and internal fluids was taken as the spraying current, standard deviation and electrowetting angle for the corresponding vegetable oil as the base fluid of external fluid.

3.3 Friction Test

Figure 4 shows the NCES friction test platform built on the CA6140A lathe. The platform was mainly composed of three parts: NCES system, loading system and data acquisition system. As shown in Figure 5, the loading system consisted of a bottom plate, a sliding rail, a slider, a collet, an auxiliary body, a spring, a bolt seat, and a loading bolt. The data acquisition system mainly included a computer and an FC3D dynamometer produced by Shanghai Naichuang Testing Technology Co., Ltd. The dynamometer was installed on the saddle of the lathe, and the loading system was installed on the dynamometer through the bottom plate.

The sliding friction test was carried out on the developed friction test platform. A YG8 carbide specimen and

Table 3 Test conditions of spraying current and electrowetting angle

Test parameters	Description
Voltage (kV)	−6.5
Total flow rate of external and internal fluids (ml/h)	15
Flow ratio of external and internal fluids Qo/Qi	1:2, 1:1, 2:1

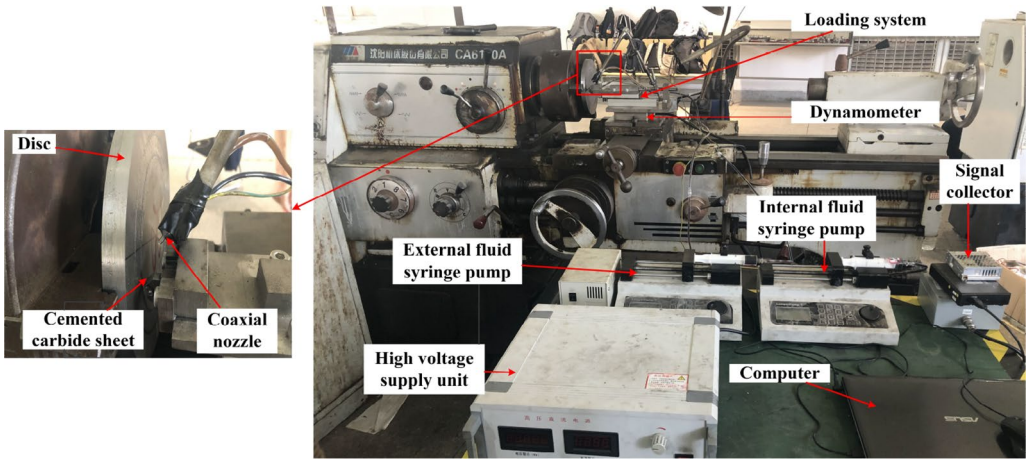

Figure 4 NCES friction test platform

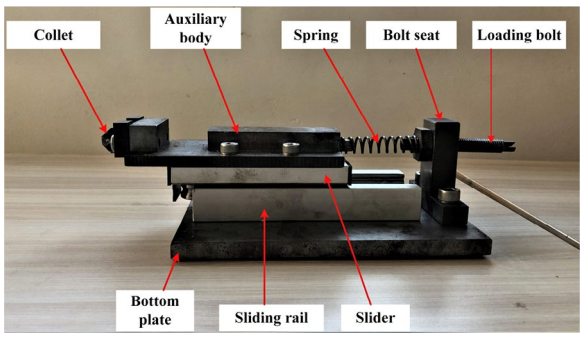

Figure 5 Loading system

Table 4 Friction test parameters

Test parameters	Description
Sliding speed (m/s)	1
Normal load (N)	30
Spraying angle (°)	35
Spraying distance (mm)	20
Voltage (kV)	−6.5
Flow rate of external fluid Qo (ml/h)	10
Flow rate of internal fluid Qi (ml/h)	5

an AISI 1045 steel disc were used as the friction pair in the test. The size and fillet radius of the carbide specimen were 12 mm×12 mm×2 mm and 0.5 mm, respectively. The size and surface roughness (Ra) of steel discs were Φ200 mm×15 mm and 0.5 μm, respectively. The carbide specimen and steel disc were installed on the collet of the loading system and the three-jaw chuck of the lathe, respectively. After the carbide specimen contacted the steel disc, the compression of the spring was changed by rotating the loading bolt so as to obtain the required normal load. The steel disc was subjected to sliding against the fillet of the carbide specimen during the test.

The friction test parameters are shown in Table 4. As shown in Figure 4, the spraying angle and distance referred to the angle between the coaxial nozzle and the steel disc and the distance between the nozzle outlet and the contact zone of the friction pair. Their values in Table 4 were applied to promote the supply of composite droplets to the friction zone. The friction time for each test was seven minutes. The three-dimensional force in the friction process was extracted and used to calculate the average value of friction force and normal load during stable friction. And the friction coefficient was obtained by using Coulomb's law. Before and after the test, the carbide specimen was ultrasonically cleaned and dried, and then the electronic analytical balance with the model FA2004B was used to weigh the mass of the carbide specimen so as to obtain the weight loss of the carbide specimen. The Olympus optical digital microscope, model DSX-500, was used to observe the surface morphology of wear mark on the steel disc. The surface morphology of wear scar on the carbide specimen was observed using a Zeiss Merlin Compact field emission scanning electron microscope (FESEM), and elementary analysis was carried out.

3.4 Milling Test

Figure 6 shows the NCES cutting test platform built on the XK714 CNC milling machine. The tool is an uncoated carbide milling cutter insert (R390-11T308M-KM H13A) manufactured by Sandvik Company, and the workpiece material is 6061 aluminum alloy with a size of 100 mm×80 mm×60 mm. The milling force and milling temperature were measured by a Kistler 9272 dynamometer and a FLIR A615 high-precision infrared thermal

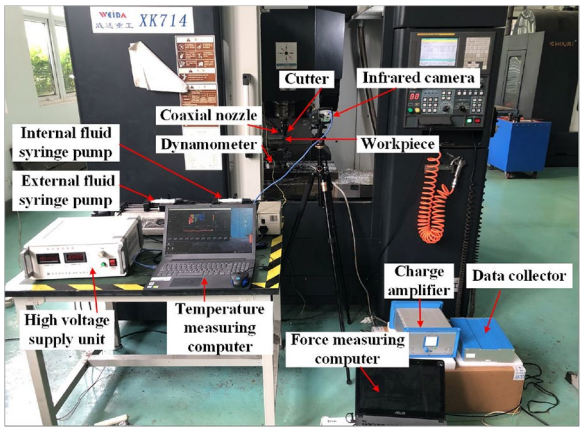

Figure 6 NCES cutting test platform

Table 5 Milling test conditions

Test parameters	Description
Milling operation	Down milling
Milling speed V_c (m/min)	196
Feed rate per tooth f_z (mm/z)	0.1
Axial depth of cut a_p (mm)	1
Radial depth of cut a_e (mm)	0.5
Spraying angle (°)	35
Spraying distance (mm)	20
Voltage (kV)	−6.5
Total flow rate of external and internal fluids (ml/h)	15
Flow ratio of external and internal fluids Qo/Qi	1:2, 1:1, 2:1

imager, respectively. Matlab software was used to calculate the average value of peak milling force in the three directions of X, Y and Z in the stable processing time, and the resultant milling force was obtained by the formula $F=(F_X^2+F_Y^2+F_Z^2)^{1/2}$. The specific milling test conditions are shown in Table 5. For effective delivery of composite droplets to the processing area, the coaxial nozzle was adjusted to the position with an angle of 35° (spraying angle) and a distance of 20 mm (spraying distance) relative to the cutter.

4 Results and Discussion

4.1 Charging and Electrowetting Properties

Figure 7 shows the effect of external/internal fluid combination on spraying current and standard deviation under different flow ratios of external and internal fluids. It can be seen that the spraying current and standard deviation with different vegetable oils as the base fluids of external fluid decreased with the increase of flow ratio of external and internal fluids. On the premise of keeping the total flow rate constant, with the increase of flow ratio of external and internal fluids, the internal fluid (water or water-based nanofluid) with good charging performance decreased, and the passive external fluid (vegetable oil or vegetable oil-based nanofluid) increased. So the spraying current and standard deviation decreased. No matter what kind of vegetable oil was used as the base fluid of external fluid in the test, because MWCNT had good conductivity, adding it to the base fluid of external or/and internal fluid generally increased the spraying current

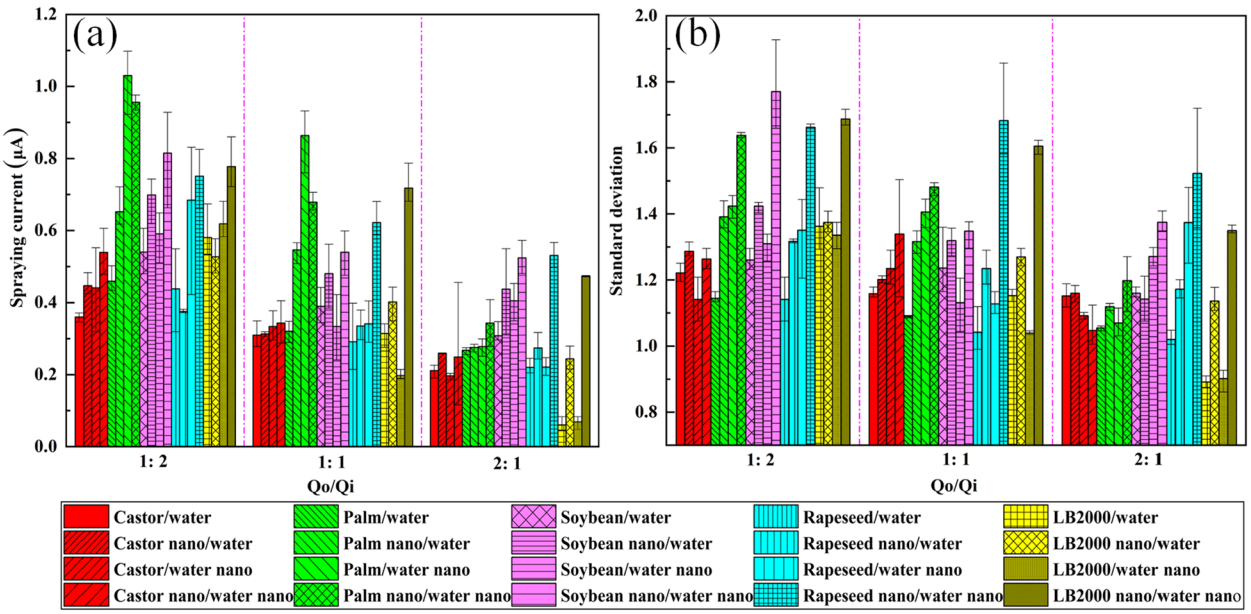

Figure 7 Spraying current and standard deviation under different flow ratios of external and internal fluids

and improved the spraying driving effect (Figure 7a). But at the same time, the addition of MWCNT also reduced the spraying resistance, namely, the interfacial tension between external and internal fluids (Table 2), which reduced the spraying stability to a certain extent and increased the standard deviation of spraying current (Figure 7b). The spraying current for the base fluid of external fluid was palm oil>soybean oil>rapeseed oil>LB2000>castor oil. The spraying stability for the base fluid of external fluid was castor oil>LB2000>palm oil>rapeseed oil>soybean oil.

Figure 8 shows the effect of external/internal fluid combination on the electrowetting angle of composite droplet under different flow ratios of external and internal fluids. It can be seen that the electrowetting angle of composite droplets with different vegetable oils as the base fluids of external fluid decreased with the increase of flow ratio of external and internal fluids. This was due to the fact that the external fluid (vegetable oil or vegetable oil-based nanofluid) with good wetting properties increased with the increase of flow ratio of external and internal fluids when the total flow rate was constant. The electrowetting angle of the composite droplets decreased as a whole when MWCNT was added to the base fluid of the external fluid. When a negative high voltage was applied to the electrode needle, the surface of the composite droplet adsorbed charges of the same polarity.

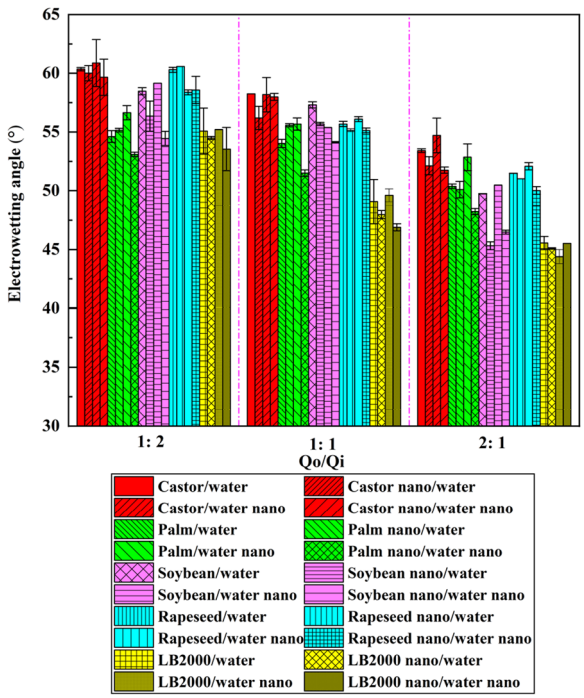

Figure 8 Electrowetting angle of composite droplet under different flow ratios of external and internal fluids

The repulsive force between charges of the same polarity reduced the surface tension of the composite droplet and enhanced the spreading properties of the composite droplet, thereby reducing the electrowetting angle. The addition of MWCNT not only helped the Brownian motion of internal molecules of vegetable oil and reduced its surface tension (Table 1), but also enhanced the charge adsorption capacity on the surface of the composite droplets and reduced the energy required for its spreading on the surface of the toughened film, thus reducing the electrowetting angle. When MWCNT was added to the base fluid of internal fluid, the electrowetting angle of the composite droplet with vegetable oil-based nanofluid as external fluid decreased. However, the electrowetting angle of the composite droplets with vegetable oil as external fluid increased. The electrowetting angle for the base fluid of external fluid was castor oil>rapeseed oil>soybean oil>palm oil>LB2000.

4.2 Friction Performance

Figure 9 shows the effect of external/internal fluid combination on friction coefficient and wear loss. It can be seen that the friction coefficient for the base fluid of external fluid was LB2000<soybean oil<palm oil<rapeseed oil<castor oil. And the wear loss of the carbide specimen for the base fluid of external fluid was LB2000<soybean oil<rapeseed oil<palm oil<castor oil. The wear loss of the carbide specimen and the friction coefficient were both the smallest when LB2000 was used as the base fluid of external fluid. With respect to NCES with other vegetable oils as the base fluids of external fluid, NCES with LB2000 as the base fluid of external fluid reduced the friction coefficient and wear loss by 9.4%–27.7% and 7.6%–26.5%, respectively. With LB2000 as the base fluid of external fluid, the spraying stability was high, and the electrowetting angle of composite droplet was the smallest. In this way, composite droplets could be stably and effectively transported and penetrate into the friction contact interface, which enhanced the cooling and lubrication performance. In addition, LB2000 had good extreme pressure performance, high oil film strength, and strong load resistance and impact resistance, effectively reducing the friction between the carbide specimen and the steel disc. Therefore, when using LB2000 as the base fluid of external fluid, the wear loss of carbide specimen and the friction coefficient were both the smallest.

Figure 10 shows the wear mark morphology of steel discs under different external/internal fluid combinations. When castor oil/water nano was used as external/internal fluid, the wear mark with the dark color on the steel disc was rough and uneven, and obvious furrows and material plastic accumulation could be seen in some areas (Figure 10b). However, when LB2000/water nano

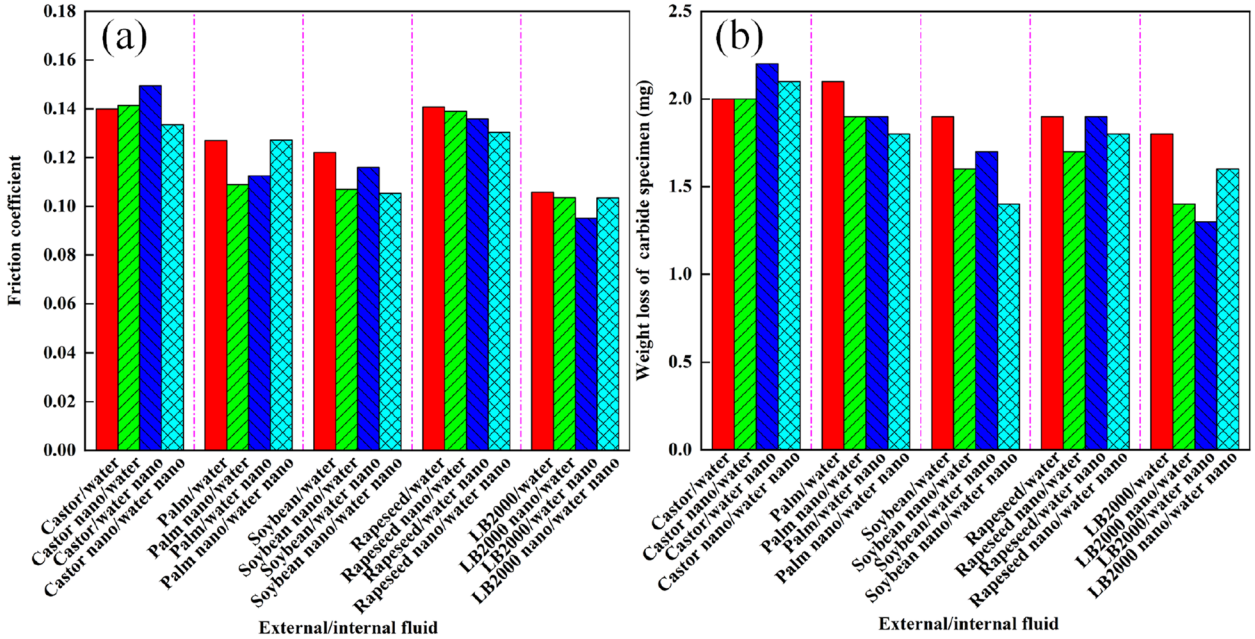

Figure 9 Effect of external/internal fluid combination on friction coefficient and wear loss

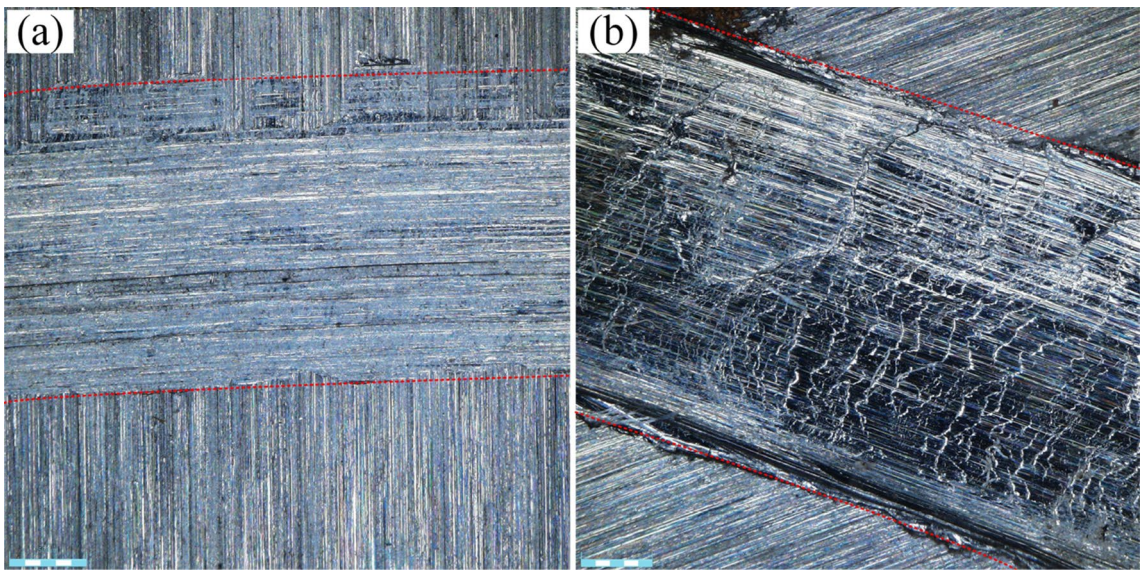

Figure 10 Wear mark morphology of steel disc: **a** LB2000/water nano, **b** Castor/water nano

was used as external/internal fluid, the wear mark with a light color on the steel disc was smooth and flat, and the furrows were not obvious (Figure 10a). Figure 11 shows the SEM photos and elementary analysis of the wear scar of the carbide specimen under different external/internal fluid combinations. When castor oil/water nano was used as external/internal fluid, there were a lot of adhering materials on the surface of the wear scar of the carbide specimen, and the corresponding elementary analysis showed a high content of Fe (Figure 11b). This indicated that the steel disc material adhered heavily to the surface of the wear scar of the carbide specimen when castor oil/water nano was used as external/internal fluid. However, when LB2000/water nano was used as external/internal fluid, high content of W and Co was found by elementary analysis (Figure 11a), indicating that the adhesion of steel disc material on the surface of wear scar of the carbide specimen was greatly reduced. These results were

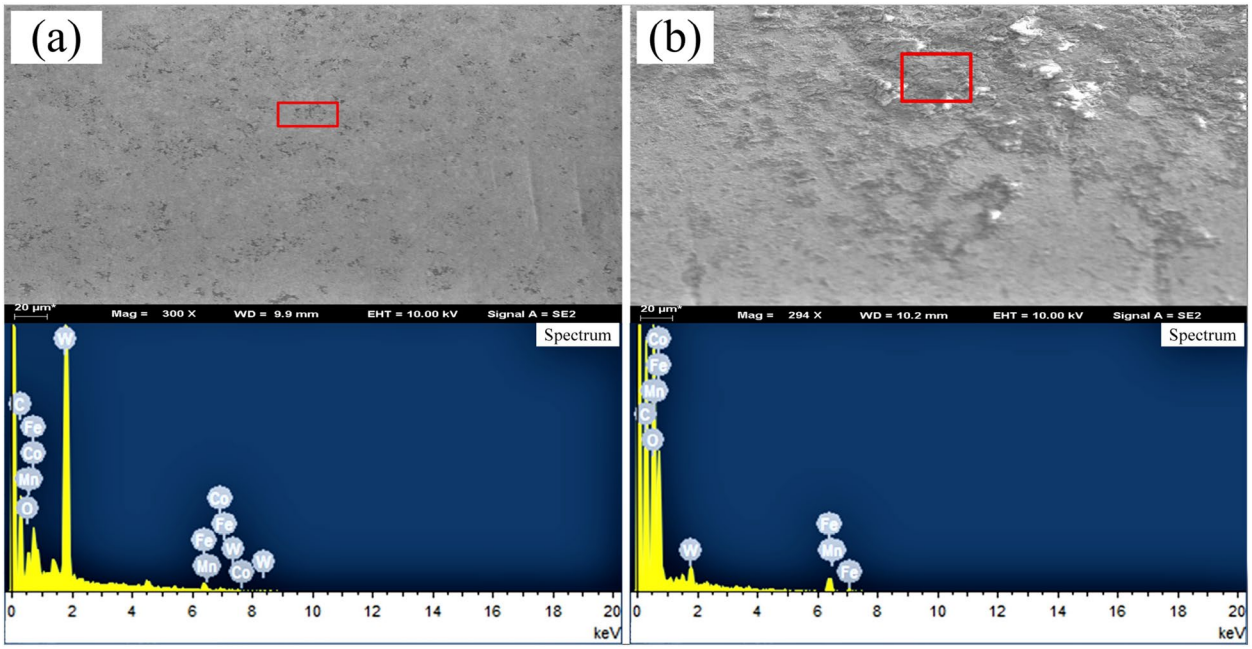

Figure 11 SEM photos and elementary analysis of wear scar of carbide specimen: **a** LB2000/water nano, **b** Castor/water nano

in line with the corresponding friction and wear behavior (Figure 9).

4.3 Milling Performance

Figure 12 shows the effect of external/internal fluid combination on milling force and milling temperature under different flow ratios of external and internal fluids. As can be seen, for the external/internal fluid combination with different vegetable oils as the base fluids of external fluid, the milling force generally decreased with the increase of flow ratio of external and internal fluids. This was due to the improvement of spraying stability, the

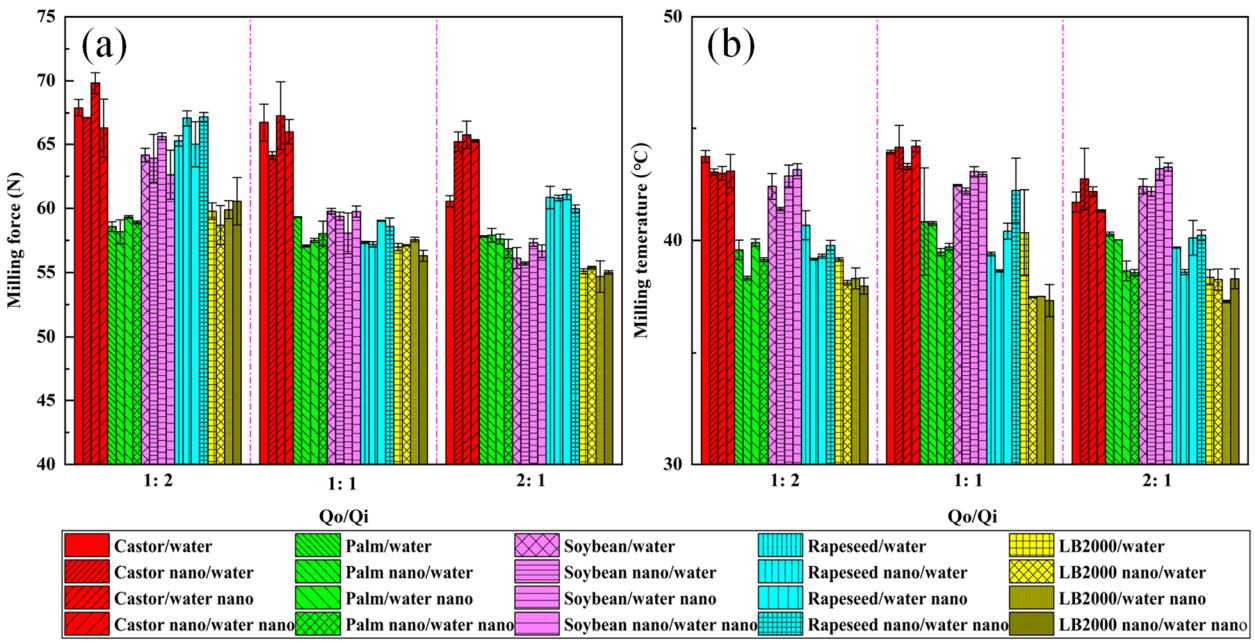

Figure 12 Milling force and milling temperature under different flow ratios of external and internal fluids

reduction of electrowetting angle of composite droplet and the increase of the amount of vegetable oil involved in lubrication caused by the increase of flow ratio of external and internal fluids. The milling force for the base fluid of external fluid was LB2000<palm oil<soybean oil<rapeseed oil<castor oil. The milling temperature for the base fluid of external fluid was LB2000<palm oil<rapeseed oil<soybean oil<castor oil. It can be seen that the milling force and milling temperature were the lowest when LB2000 was used as the base fluid of external fluid, and the milling force and milling temperature were the highest when castor oil was used as the base fluid of external fluid. The milling force and milling temperature for NCES with LB2000 as the base fluid of external fluid were 1.4%-13.2% and 3.6%-11.2% lower than those for NCES with other vegetable oils as the base fluids of external fluid, respectively.

The composition and viscosity of vegetable oil were important factors affecting its cooling and lubricating properties. Vegetable oils were mainly composed of triglycerides and fatty acids. Further, fatty acids were divided into saturated fatty acids, monounsaturated fatty acids containing one unsaturated bond, and polyunsaturated fatty acids containing two or more unsaturated bonds. The presence of unsaturated bonds reduced the strength of the lubricating film and the oxidative stability of vegetable oil. Therefore, vegetable oils with higher saturated fatty acid content exhibited higher lubricating film strength than those with higher unsaturated fatty acid content. The lubricating oil film strength formed by monounsaturated fatty acids was higher than that formed by polyunsaturated fatty acids. In addition, since the total adsorption energy of vegetable oil increased with the increase of the number of carbon atoms in the fatty acid, the increase of carbon chain length of fatty acid was beneficial to improve the oil film strength. The fatty acid composition of different vegetable oils is shown in Table 6. Among them, palmitic acid, stearic acid and eicosanoic acid were saturated fatty acids; oleic acid, ricinoleic acid and erucic acid were monounsaturated fatty acids, and linoleic acid and linolenic acid were polyunsaturated fatty acids. The main functional groups of LB2000 oil droplets were measured by Fourier transform infrared spectroscopy. The results showed that the main fatty acids of LB2000 were oleic acid and linoleic acid [35]. The molecular structure of typical fatty acids in vegetable oils used in the test is shown in Figure 13. The viscosities of different vegetable oils and their oil-based nanofluids are listed in Table 1. It can be seen that when MWCNT was added to vegetable oil, the viscosity increased. Furthermore, the viscosity of castor oil and its oil-based nanofluids was more than 10 times that of other vegetable oils and their oil-based nanofluids. The vegetable oil with high viscosity had poor flow performance so that it was difficult to penetrate into the processing area, while the vegetable oil with low viscosity could easily penetrate into the processing area, take away heat and realize lubrication. However, with the decrease of viscosity, the strength of lubricating oil film formed on the surfaces of cutting tool and workpiece decreased.

The excellent spraying stability, electrowetting property and LB2000 lubrication performance led to the lowest milling force and milling temperature with LB2000 as the base fluid of the external fluid. The content of ricinoleic acid in castor oil was more than 90% (Table 6), and the ricinoleic acid contained two polar groups, namely, carboxyl (-COOH) and hydroxyl (-OH) (Figure 13c), which made castor oil have strong adsorption capacity on the metal surface and easy to form the lubricating oil film. However, the spraying current with castor oil as the base fluid of external fluid was the smallest, and the surface

Table 6 Fatty acid composition of different vegetable oils [17]

Fatty acid (%)	Castor oil	Palm oil	Soybean oil	Rapeseed oil
Palmitic acid	0.72	45.1	8.9	2.63
Stearic acid	0.64	4.8	3.8	11.72
Oleic acid	2.82	36.8	23	5.92
Linoleic acid	3.74	10.2	52.4	23.63
Linolenic acid	–	–	10.6	3.34
Ricinoleic acid	90.85	–	–	–
Eicosanoic acid	–	–	–	2.92
Erucic acid	-	–	–	43.63

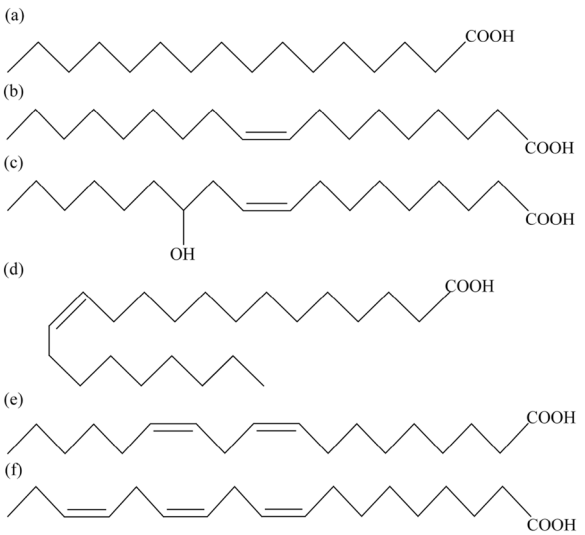

Figure 13 Molecular structure: **a** Palmitic acid, **b** Oleic acid, **c** Ricinoleic acid, **d** Erucic acid, **e** Linoleic acid and **f** Linolenic Acid

tension and viscosity of castor oil were large (Table 1), resulting in the composite droplets with large size and slow conveying speed. In this way, the composite droplets were easy to be affected by the air flow field around the milling cutter. In addition, the electrowetting angle of composite droplets with castor oil as the base fluid of external fluid was the largest. All these made it difficult for composite droplets to transport and penetrate into the processing area. So the milling force and milling temperature with castor oil as the base fluid of external fluid were the highest.

With palm oil as the base fluid of external fluid, the spraying current was the largest, and more fine composite droplets could be quickly transported to the processing area under the action of electric field force. In addition, the composite droplet with palm oil as the base fluid of external fluid had a small electrowetting angle and a large wetting area, which was beneficial to its penetration into the processing area and the exertion of its cooling and lubricating effects. At the same time, palm oil contained nearly 50% saturated fatty acids (palmitic acid and stearic acid), and thus presented higher strength and oxidative stability of oil film than soybean oil and rapeseed oil. Therefore, the milling force and milling temperature with palm oil as the base fluid of external fluid were lower than those with rapeseed oil and soybean oil as the base fluid of external fluid.

Soybean oil contained more than 50% linoleic acid (polyunsaturated fatty acid), while rapeseed oil contained more than 40% erucic acid (monounsaturated fatty acid) with carbon chain length of 22. So the strength and oxidative stability of oil film with rapeseed oil as the base fluid of external fluid were higher than those with soybean oil as the base fluid of external fluid. However, due to higher spraying current and smaller electrowetting angle, the transport and permeability of composite droplets with soybean oil as the base fluid of external fluid were better than those with rapeseed oil as the base fluid of external fluid. Therefore, the milling force with soybean oil as the base fluid of external fluid was lower than that with rapeseed oil as the base fluid of external fluid. In addition, the thermal conductivity of vegetable oil decreased with the increase of linolenic acid content. The linolenic acid content in soybean oil was higher than that in rapeseed oil, which made the milling temperature with soybean oil as the base fluid of external fluid higher than that with rapeseed oil as the base fluid of external fluid.

Compared with castor oil, soybean oil, palm oil, and rapeseed oil, LB2000 was more suitable as the base fluid of external fluid for NCES cutting. Further, when the external/internal fluid was LB2000/water nano and the flow ratio of external and internal fluids was 2:1, the minimum milling force and milling temperature were gained. This was attributed to excellent spraying stability, electrowetting performance, and synergistic heat transfer and friction reduction efficiency of MWCNT.

5 Conclusions

Although NCES was an effective MQL improvement technology, it was unclear which base fluid of external fluid was the most conducive to the performance of NCES. In this work, the friction and milling performances of NCES with different vegetable oils as the base fluids of external fluid were compared under different flow ratios of external and internal fluids to determine the suitable base fluid of external fluid. The spraying current, standard deviation, and electrowetting angle were tested to analyze the charging performance, spraying stability, and electrowetting property of NCES with different vegetable oils as the base fluids of external fluid. And the influence of vegetable oil type as the base fluid of external fluid on NCES performances was discussed. The following conclusions can be drawn.

(1) The spraying current with different vegetable oils as the base fluids of external fluid was ranked as palm oil>soybean oil>rapeseed oil>LB2000>castor oil. The spraying stability with different vegetable oils as the base fluids of external fluid was ranked as castor oil>LB2000>palm oil>rapeseed oil>soybean oil. The electrowetting properties of composite droplets with different vegetable oils as the base fluids of external fluid were ranked as LB2000>palm oil>soybean oil>rapeseed oil>castor oil.
(2) When castor oil was used as the base fluid of external fluid, NCES presented the worst antifriction and antiwear performance, while when LB2000 was used as the base fluid of external fluid, NCES showed the best antifriction and antiwear performance. Especially when LB2000/water nano was used as external/internal fluid, the minimum wear loss of carbide specimen and friction coefficient could be obtained. Besides it, the wear mark on the steel disc was smooth and flat, and the steel disc material rarely adhered to the wear scar of carbide specimen.
(3) Owing to excellent spraying stability, electrowetting property and LB2000 lubrication performance, LB2000 was more suitable as the base fluid of external fluid for NCES cutting than other vegetable oils, which could effectively reduce the milling force and milling temperature. The optimal external/internal fluid combination and flow ratio of external and internal fluids were LB2000/water nano and 2:1 to obtain the minimum milling force and milling temperature.

Acknowledgements
Not applicable.

Author Contributions
YS wrote and revised the manuscript. ZC and BW conducted the experiments and drew the graphs and charts. LG performed the data analysis. ZL reviewed and edited the manuscript. All authors read and approved the final manuscript.

Authors' Information
Yu Su, born in 1979, is a professor at *College of Mechanical Engineering, Jiangsu University of Science and Technology, China*. His research interests include green machining of difficult-to-cut materials, high-speed cutting and tool coating.
Zepeng Chu, born in 1997, is a master candidate at *College of Mechanical Engineering, Jiangsu University of Science and Technology, China*.
Le Gong, born in 1988, is a lecturer at *College of Mechanical Engineering, Jiangsu University of Science and Technology, China*. His main research interests include green machining and surface integrity.
Bin Wang, born in 1998, is a master candidate at *College of Mechanical Engineering, Jiangsu University of Science and Technology, China*.
Zhiqiang Liu, born in 1979, is a professor at *College of Mechanical Engineering, Jiangsu University of Science and Technology, China*. His research interests are mainly focused on high-efficiency machining of titanium alloys and micro milling.

Funding
Supported by National Natural Science Foundation of China (Grant Nos. 52175411 and 51205177) and Jiangsu Provincial Natural Science Foundation (Grant Nos. BK20171307 and BK2012277).

Data availability
The datasets used and/or analysed during the current study are available from the corresponding author on reasonable request.

Declarations

Competing Interests
The authors declare no competing financial interests.

Received: 17 July 2022 Revised: 26 July 2023 Accepted: 27 July 2023
Published online: 24 August 2023

References

[1] W H Xu, C H Li, Y B Zhang, et al. Electrostatic atomization minimum quantity lubrication machining: from mechanism to application. *International Journal of Extreme Manufacturing*, 2022, 4: 042003.
[2] Y Cao, J F Yin, W F Ding, et al. Alumina abrasive wheel wear in ultrasonic vibration-assisted creep-feed grinding of Inconel 718 nickel-based superalloy. *Journal of Materials Processing Technology*, 2021, 297: 117241.
[3] Q Miao, W F Ding, J H Xu, et al. Creep feed grinding induced gradient microstructures in the superficial layer of turbine blade root of single crystal nickel-based superalloy. *International Journal of Extreme Manufacturing*, 2021, 3: 045102.
[4] Y Cao, Y J Zhu, W F Ding, et al. Vibration coupling effects and machining behavior of ultrasonic vibration plate device for creep-feed grinding of Inconel 718 nickel-based superalloy. *Chinese Journal of Aeronautics*, 2022, 35(2): 332-345.
[5] W J Kuang, Q Miao, W F Ding, et al. Fretting wear behaviour of machined layer of nickel-based superalloy produced by creep-feed profile grinding. *Chinese Journal of Aeronautics*, 2022, 35(10): 401-411.
[6] G M Krolczyk, R W Maruda, J B Krolczyk, et al. Ecological trends in machining as a key factor in sustainable production–A review. *Journal of Cleaner Production*, 2019, 218: 601-615.
[7] L Z Tang, Y B Zhang, C H Li, et al. Biological stability of water-based cutting fluids: progress and application. *Chinese Journal of Mechanical Engineering*, 2022, 35: 3.
[8] R Sankaranarayanan, N Rajesh Jesudoss Hynes, J Senthil Kumar, et al. A comprehensive review on research developments of vegetable-oil based cutting fluids for sustainable machining challenges. *Journal of Manufacturing Processes*, 2021, 67: 286-313.
[9] B Sen, M Mia, G M Krolczyk, et al. Eco-friendly cutting fluids in minimum quantity lubrication assisted machining: a review on the perception of sustainable manufacturing. *International Journal of Precision Engineering and Manufacturing-Green Technology*, 2021, 8: 249-280.
[10] X Cui, C H Li, W F Ding, et al. Minimum quantity lubrication machining of aeronautical materials using carbon group nanolubricant: from mechanisms to application. *Chinese Journal of Aeronautics*, 2022, 35(11): 85-112.
[11] B Boswell, M N Islam, I J Davies, et al. A review identifying the effectiveness of minimum quantity lubrication (MQL) during conventional machining. *International Journal of Advanced Manufacturing Technology*, 2017, 92: 321-340.
[12] Y B Zhang, H N Li, C H Li, et al. Nano-enhanced biolubricant in sustainable manufacturing: from processability to mechanisms. *Friction*, 2022, 10(6): 803-841.
[13] K K Gajrani, M R Sankar. Past and current status of eco-friendly vegetable oil based metal cutting fluids. *Materials Today Proceedings*, 2017, 4: 3786-3795.
[14] Y G Wang, C H Li, Y B Zhang, et al. Experimental evaluation of the lubrication properties of the wheel/workpiece interface in minimum quantity lubrication (MQL) grinding using different types of vegetable oils. *Journal of Cleaner Production*, 2016, 127: 487-499.
[15] I Deiab, S W Raza, S Pervaiz. Analysis of lubrication strategies for sustainable machining during turning of titanium Ti-6Al-4V alloy. *Procedia CIRP*, 2014, 17: 766-771.
[16] M H S Elmunafi, D Kurniawan, M Y Noordin. Use of castor oil as cutting fluid in machining of hardened stainless steel with minimum quantity of lubricant. *Procedia CIRP*, 2015, 26: 408-411.
[17] B K Li, C H Li, Y B Zhang, et al. Grinding temperature and energy ratio coefficient in MQL grinding of high-temperature nickel-base alloy by using different vegetable oils as base oil. *Chinese Journal of Aeronautics*, 2016, 29(4): 1084-1095.
[18] M Z Liu, C H Li, Y B Zhang, et al. Cryogenic minimum quantity lubrication machining: from mechanism to application. *Frontiers of Mechanical Engineering*, 2021, 16(4): 649-697.
[19] K C Wickramasinghe, H Sasahara, E A Rahim, et al. Recent advances on high performance machining of aerospace materials and composites using vegetable oil-based metal working fluids. *Journal of Cleaner Production*, 2021, 310: 127459.
[20] K Zadafiya, P Shah, A Shokrani, et al. Recent advancements in nano-lubrication strategies for machining processes considering their health and environmental impacts. *Journal of Manufacturing Processes*, 2021, 68: 481-511.
[21] K Manojkumar, A Ghosh. Assessment of cooling-lubrication and wettability characteristics of nano-engineered sunflower oil as cutting fluid and its impact on SQCL grinding performance. *Journal of Materials Processing Technology*, 2016, 237: 55-64.
[22] Y B Zhang, C H Li, M Yang, et al. Experimental evaluation of cooling performance by friction coefficient and specific friction energy in nanofluid minimum quantity lubrication grinding with different types of vegetable oil. *Journal of Cleaner Production*, 2016, 139: 685-705.
[23] Y B Zhang, C H Li, D Z Jia, et al. Experimental evaluation of MoS_2 nanoparticles in jet MQL grinding with different types of vegetable oil as base oil. *Journal of Cleaner Production*, 2015, 87: 930-940.
[24] S M Yuan, X B Hou, L Wang, et al. Experimental investigation on the compatibility of nanoparticles with vegetable oils for nanofluid minimum quantity lubrication machining. *Tribology Letters*, 2018, 66: 106.
[25] A Pal, S S Chatha, H S Sidhu. Experimental investigation on the performance of MQL drilling of AISI 321 stainless steel using nano-graphene enhanced vegetable-oil-based cutting fluid. *Tribology International*, 2020, 151: 106508.
[26] H Singh, V S Sharma, M Dogra. Exploration of graphene assisted vegetables oil based minimum quantity lubrication for surface grinding of TI-6AL-4V-ELI. *Tribology International*, 2020, 144: 106113.
[27] Y Su, L Gong, B Li, et al. Performance evaluation of nanofluid MQL with vegetable-based oil and ester oil as base fluids in turning. *International Journal of Advanced Manufacturing Technology*, 2016, 83: 2083-2089.

[28] N S K Reddy, M Yang. Development of an electro static lubrication system for drilling of SCM 440 steel. *Proceedings of the Institution of Mechanical Engineers, Part B: Journal of Engineering Manufacture*, 2010, 224(2): 217-224.
[29] N S K Reddy, M Nouari, M Y Yang. Development of electrostatic solid lubrication system for improvement in machining process performance. *International Journal of Machine Tools and Manufacture*, 2010, 50: 789-797.
[30] Y Su, Q Lu, T Yu, et al. Machining and environmental effects of electrostatic atomization lubrication in milling operation. *International Journal of Advanced Manufacturing Technology*, 2019, 104: 2773-2782.
[31] Y Su, H Jiang, Z QLiu. A study on environment-friendly machining of titanium alloy via composite electrostatic spraying. *International Journal of Advanced Manufacturing Technology*, 2020, 110: 1305-1317.
[32] Y Su, W H Gao, H Jiang, et al. Experimental investigation on the performance of composite electrostatic spraying milling using different inner/outer fluid combinations. *Machining Science and Technology*, 2021, 25(6): 1010-1030.
[33] JM López-Herrera, A Barrero, A López,et al. Coaxial jets generated from electrified Taylor cones. Scaling laws. *Journal of Aerosol Science*, 2003, 34: 535-552.
[34] Y Su, XR Hu, DD Zhang, et al. Performance evaluation of composite electrostatic spraying (CES) in milling process. *International Journal of Advanced Manufacturing Technology*, 2021, 117: 109-123.
[35] S Q Huang. *A study on lubrication-cooling mechanisms and machining characteristics of electrostatic minimum quantity lubrication (EMQL)*. Hangzhou: Zhejiang University of Technology, 2018. (in Chinese)